UNIVERSITY OF CALIFORNIA, SAN DIEGO

Ablation of Inducible Nitric Oxide Synthase does not alter Alzheimer's like Pathology in Transgenic Mice

A Thesis submitted in partial satisfaction of the requirements for the degree Master of Science

in

Biology

by

Timothy Shane Foster

Committee in charge:

Professor Edward Koo, Chair
Professor Gentry Patrick, Co-Chair
Professor Randolph Hampton

2012

The thesis of Timothy Shane Foster is approved and it is acceptable in quality and form for publication on microfilm and electronically

_____

_____
Co-Chair

_____
Chair

University of California, San Diego

2012

TABLE OF CONTENTS

LIST OF FIGURES

ACKNOWLEDGEMENTS

I would like to thank Professor Edward Koo for his support and advice throughout this process. I would also like to thank him for allowing me to be a part of this wonderful lab. I would also like to especially thank Dr. Aimee Pierce who taught me all of the techniques needed for this study. Her guidance and help throughout the project was very much appreciated.

In addition, I would like to thank the entire Koo Lab for their help. I would also like to thank Floyd Sarsoza and Hiroko Maruyama who helped me perform the experiments.

ABSTRACT OF THE THESIS

Ablation of Inducible Nitric Oxide Synthase does not alter Alzheimer's-like Pathology in Transgenic Mice

by

Timothy Shane Foster

Master of Science in Biology

University of California, San Diego, 2012

Professor Edward Koo, Chair
Professor Gentry Patrick, Co-Chair

The progression of Alzheimer's disease is theorized to progress from amyloid pathology to tau pathology as shown in the amyloid cascade hypothesis. The pathway for this progression is, as of yet, unknown. Previous studies have shown a correlation between the presence of inducible nitric oxide synthase and the severity of Alzheimer's disease mouse models. Using mice carrying mutations in the amyloid precursor protein crossed with mice lacking inducible nitric oxide synthase we examined the link between disease progression and the presence of nitric oxide synthase. Additionally, mice carrying the amyloid precursor protein (APP) mutation in conjunction with a mutation in the caspase cleavage domain of APP were studied in the context of the ablation of inducible nitric oxide synthase. The mice were evaluated

in terms of amyloid plaque load, levels of amyloid beta protein, and levels of hyperphosphorylated tau protein. There was no obvious correlation between the ablation of inducible nitric oxide synthase and the severity of Alzheimer's-like pathology. Mice carrying the caspase cleavage mutation showed a significant increase in amyloid plaque load when completely lacking inducible nitric oxide synthase compared to mice carrying the same mutations but with one copy of the inducible nitric oxide synthase gene.

INTRODUCTION

Alzheimer's Disease Overview, Risk Factors and Treatments:

Neurodegenerative disorders are a prevalent cause of death in the world today affecting more than 34 million people worldwide (Wimo et al, 2010). These neurodegenerative diseases are characterized by a progressive deterioration of the nervous system mediated by loss of synaptic function and/or neuronal death. This degeneration results in dementia (Goedert et al, 1998). It has been estimated that the worldwide cost of dementia treatments totaled $422 billion in 2009 alone. If informal care is taken into account the estimate can range as high as $608 billion, with each case costing an average of $36,000 in North America (Wimo et al, 2010). Dementia is defined as a decline in memory coupled with a deficit in at least one other faculty. Specifically aphasia, apraxia, agnosia, or a decrease in executive function severe enough to interfere with activities of daily life must be observed in conjunction with memory loss (DSM IV).

Although there are many neurodegenerative diseases, notably Parkinson's disease and Creutzfeldt-Jakob disease, the most common neurodegenerative disease is Alzheimer's disease. Alzheimer's disease (AD) accounts for approximately 60% of dementia cases worldwide. It is estimated that 5.4 million Americans have Alzheimer's disease, with the majority of those aged 65 years or older (5.2 million). Additionally 13% of the population over 65 has Alzheimer's disease and the number of Americans over 65 with Alzheimer's is expected to increase to between 11 and 16 million by the year 2050. Furthermore, the prevalence of the disease is expected to rise

greatly in the coming years, largely due to the expected increase in the percentage of the population over age 65 (Alzheimer's Association, 2011)

Symptoms of Alzheimer's disease are typical of dementia. These symptoms include memory loss, difficulty solving problems, confusion, mood and personality changes which can result in the loss of the ability to perform daily activities. There are several known risk factors for Alzheimer's disease. A family history of Alzheimer's disease, specifically among first-degree relatives, presents an increased incidence of the disease (Mayeux et al, 1991). Other risk factors include obesity, diabetes mellitus, high blood pressure and high cholesterol (Kivipelto et al, 2005)(Xu et al, 2011)(Tsivgoulis et al, 2009). Smoking and traumatic brain injuries have also been found to increase the risk of Alzheimer's disease and other dementias (Antsey et al, 2007)(Lye et al, 2000**).** Another significant risk factor associated with Alzheimer's disease is the presence of the ApoE4 form of the ApoE gene, which has been shown to promote clearance of amyloid beta (Alzheimer's Association, 2011)(Cramer et al, 2012). It has also been shown that a diet high in fruits and vegetables may offer a protective phenotype (Polidori, 2009). However, despite many known risk factors, with the exception of rare forms of familial AD (including presinilin and APP mutations) that account for approximately 1% of all Alzheimer's cases, there is no known cause of the disease (Alzheimer's Association, 2011).

Although there are currently greater than 75 experimental treatments involved in clinical trials there are no proven treatments that alter the course of AD or attenuated the neurodegeneration that occurs in the brain. In particular, although there

are many experimental treatments that have been successful in rodent models, none have translated to humans in subsequent trails. There are several treatments that have been shown to slow the symptoms of Alzheimer's for up to 1 year including acetylcholinesterase inhibitors (Golde et al, 2011). Many researchers are currently focusing on improving diagnostic techniques in order to treat Alzheimer's before the onset of clinical symptoms. This chiefly involves the use of biomarkers in plasma, the brain and the cerebrospinal fluid (Alzheimer's Association, 2011). Many clinical drugs target the amyloid-beta protein though none have shown success (Salamone, 2011). Other therapies have targeted the tau protein, aimed to increase the activity of nicotinic acetylcholine receptors or have taken a wholly neuroprotective approach (Salloway, 2008).

Pathological Hallmarks of Alzheimer's Disease:

There are two major pathological hallmarks in the brain of an Alzheimer's patient. These are senile plaques and neurofibrillary tangles (NFTs) (Markesbery, 1997) (Figure 1). Senile plaques are composed of a core of amyloid-beta (Aβ) peptides and later come to incorporate parts of dead neurons and glial cells (Goedert et al, 1998). The Aβ peptides are a product of the amyloid precursor protein (APP). APP is a transmembrane protein whose principal function is unclear. There are several different isoforms of APP (due to variable splicing) and the three most common forms are 695 amino acids, 751 amino acids, and 770 amino acids (O'Brien et al, 2011). The processing of APP begins with cleavage by either α or β-secretase. From there cleavage by γ-secretase produces p3 and AICD (APP intracellular domain) in the α-

secretase pathway**,** and Aβ and AICD in the β-secretase pathway (O'Brien, 2011) (Figure 2).

The second major pathological hallmark observed in Alzheimer's disease is the NFTs, which are composed of hyperphosphorylated tau protein. The tau protein is typically a microtubule associated protein**,** but in disease states forms large aggregates inside the cell. In addition to hyperphosphorylation, some truncated tau protein has also been observed in Alzheimer's brains. It has been found that the levels of tau inclusions in an Alzheimer's brain correspond well with the severity of the disease-something that cannot be said for Aβ load. It is believed that in the disease state tau gains a toxic function in the neurons (Binder et al, 2005).

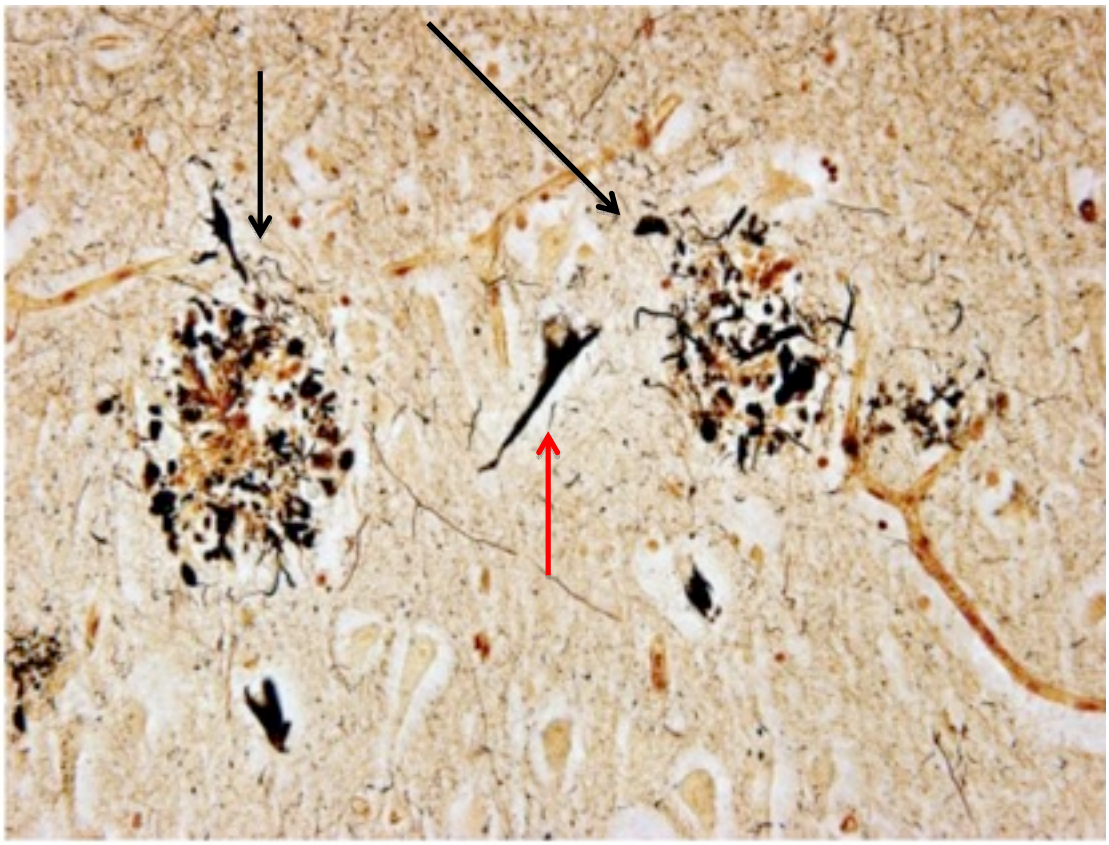

Figure 1: Example of amyloid plaques and neurofibrillary tangles

An image of representative AD pathology. This is a Bielschowski stain showing amyloid plaques (black arrows) and a neurofibrillary tangle (red arrow). This image is adapted from Perl et al, 2010.

Amyloid Cascade Hypothesis:

One of the most popular current hypotheses regarding Alzheimer's disease is known as the amyloid cascade hypothesis. The hypothesis posits that the accumulation of Aβ peptides is the initiating step in Alzheimer's progression. The Aβ peptides form oligomers that initiate a cascade of events that result in the full spectrum of AD pathology. Specifically, Aβ oligomers are believed to promote the aggregation of microglial cells and activate inflammatory pathways. In part, these steps are thought to lead to the formation of neurofibrillary tangles and neuronal loss through a pathway that remains unknown (Hardy et al, 2002). It has been hypothesized that the accumulation of Aβ that initiates the disease may begin as early as 10 years prior to the earliest clinical symptoms (Golde et al, 2011).

One theory regarding the progression from Aβ pathology to tau pathology and neuronal loss involves the use of APP as a receptor for fibrillar Aβ. As evidence for this theory it has been found that neurons lacking APP were less susceptible to Aβ toxicity than wild type neurons (Lorenzo, 2000). It has also been shown that Aβ causes the caspase-mediated cleavage of APP at amino acid 664 to produce a C-terminal fragment of 31 amino acids termed C31 (Lu et al, 2003). Furthermore, C31 had previously been shown to have neurotoxic effects of its own (Lu et al, 2000). Additionally, the toxic effects of both Aβ and C31 were attenuated in the absence of APP (Lu et al, 2003). Blockage of the caspase cleavage site by the mutation D664A ameliorated the toxic effects of both C31 and Aβ (Lu et al, 2000)(Lu et al, 2003). It has also been shown that this cleavage at amino acid 664 and activation of caspase-9

occurs in the brains of Alzheimer's patients (Lu et al, 2000). This data all indicates that Aβ toxicity proceeds through interaction with APP and the generation of the C31 fragment.

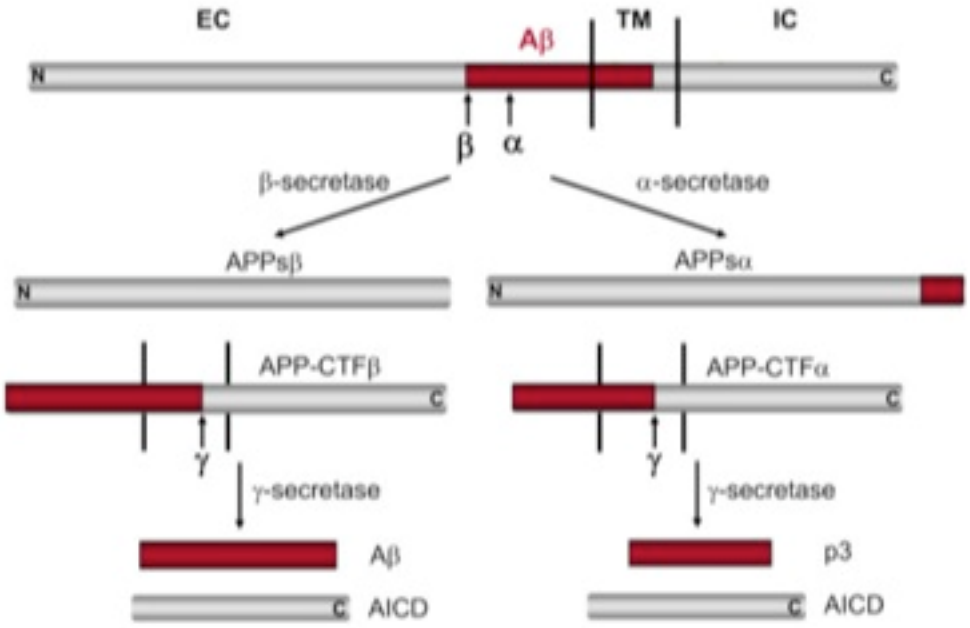

Figure 2: A schematic of APP processing pathways

This is a schematic of the variable processing pathways for APP. The red area is representative of the Aβ region of APP. The pathway on the left is termed amyloidogenic while the pathway on the left is the non-amyloidogenic pathway. This figure is adapted from Zheng and Koo, 2011.

J20 and B21 Mice:

Transgenic mice carrying mutated forms of human APP are commonly used as models for Alzheimer's disease research. The lines are designed to express APP with a predisposition towards the production and deposition of amyloid beta. The J20 (APPSwInd) transgenic mouse line, one of the more popular lines, was created by introducing the Swedish mutation (K670N, M671L) and Indiana mutation (V717F) in the human APP cDNA. Expression of the hAPP was driven by the PDGFβ promoter (Hsia, 1999). It has been shown that J20 mice produced levels of hAPP similar to those observed in the H6 line, the latter expressing only the "Indiana" mutation. However the J20 line produced greater levels of Aβ42 and developed plaques in the hippocampal regions of the brain much earlier than the H6 mice (Mucke, 2000). Additionally, it has been shown that J20 mice do not have deficits in short-term memory, short-term object recognition or in fear conditioning tasks. The mice do exhibit deficits in spatial memory (Karl et al, 2012).

The B21 (APPSwInd D664A) mouse line was derived using the same construct used in generating the J20 line described above except for the addition of a D664A mutation that abrogates caspase cleavage site of APP. In comparison to J20 mice, B21 mice do not show a deficit in basal synaptic transmission. Instead B21 mice showed synaptic function comparable to that of normal wild-type non-transgenic mice. Additionally, no deficits were observed in long-term potentiation in the B21 mice. In contrast, J20 mice exhibited a significant decrease in the ability to perform long-term potentiation. Furthermore, J20 mice showed learning deficits at 8-12 months of age

that were absent in B21 mice. Interestingly, APP expression, amyloid levels and senile plaque formation did not differ between the lines indicating that the D664A mutation did not alter the production of Aβ (Saganich et al, 2006). These findings have been interpreted to indicate that the progression of AD is dependent on caspase-mediated cleavage of APP.

Limitations of Current Mouse Models:

Current mouse models of Alzheimer's disease do not fully recreate the pathology of Alzheimer's. Mice that carry a mutated human APP transgene develop plaques, amyloid pathology and behavioral deficits (Hsiao et al, 1996). However, they do not progress to the tau pathology observed in Alzheimer's patients. In order to display pathology that more resembles AD, a mutated form of tau transgene must also be expressed (Oddo et al, 2003). Mutated tau protein is common in frontal temporal dementia cases, but not in Alzheimer's cases (Iqbal, 2005). Therefore, the use of mutated tau isoforms to mimic Alzheimer's disease does not accurately depict the normal biology of the disease. In some aspects it is beneficial to have incomplete mouse models. It allows for isolation of certain aspects of the disease and offers easier access to testing theories regarding those pathologies (Radde, 2008). However, a more complete mouse model is needed in order to take a more holistic view of Alzheimer's disease. A model is needed that progresses naturally from amyloid pathology to tau pathology without mutating tau.

Nitric Oxide:

Nitric oxide is a molecule involved in many different processes in the body [(Nathan, 1994)(Nathan, 1992)(Moncada, 1993). It is principally a neurotransmitter and intercellular mediator (Vincent, 1994). Nitric oxide is synthesized from L-arginine by the enzyme nitric oxide synthase (NOS), which is found in three different isoforms. These isoforms are neuronal NOS (type I), inducible NOS (type II) and endothelial NOS (type III). Both nNOS and eNOS are constitutively expressed throughout the brain (Fernandez, 2010).

Another role that nitric oxide is known to play in the body is related to inflammation. Nitric oxide is released from glial cells, along with other factors, during brain tissue inflammation (Hartlage-Rubsamen, 2001). In fact, excess nitric oxide (presumably from iNOS) has been shown to be neurotoxic and pro-inflammatory (Wallace, 1997). This is significant because inflammation has been implicated in Alzheimer's disease (McGeer, 1999). In addition, Aβ increases nitric oxide production in neurons (Hu, 1993). It has also been found that increased iNOS reactivity is associated with tangle-bearing neurons in the brains of Alzheimer's patients (Vodovotz, 1996). Together, these results indicate that inducible nitric oxide synthase may play a significant role in the progression of Alzheimer's disease.

Mice Deficient in NOS2 Carrying a Mutated APP Gene:

Keeping in mind the potential links between nitric oxide and Alzheimer's disease mice carrying mutated human APP were crossed with mice deficient in inducible nitric oxide synthase (NOS2). Colton et al found that APPSw/NOS2-/- mice had elevated levels of phosphorylated tau as determined by probing with an antibody

recognizing phosphorylated tau at serine 202 and threonine 205 (AT8), in comparison to mice carrying the APP mutation alone. These findings were shown in western blots and by way of immunohistochemistry. Additionally it was shown that APPSwNOS-/- mice had elevated levels of insoluble Aβ when compared to APPSw mice. The study also showed that degenerating neurons were present in the brains of APPSwNOS2-/- mice**,** but were absent in the brains of APPSw and wild type mice.

Follow up studies by the same group corroborated many of the earlier results: increased levels of hyperphosphorylated tau (Wilcock, 2009) and increased Aβ plaque load (Colton, 2009) were replicated. Additionally, both studies reported behavior and learning deficits in the mice carrying an APP mutation and lacking NOS2. Neuronal loss was also shown in the mice compared to APPSw mice (Colton, 2009)(Wilcock, 2009). Furthermore, neuropeptide Y neuron loss was observed (Wilcock, 2009). Taken together, these results led to the conclusion that the ablation of inducible nitric oxide synthase led to a more severe mouse model of Alzheimer's disease. The presence of hyperphosphorylated tau (at serine 202/threonine 205), as shown by AT8 immunohistochemistry, was taken to indicate a natural progression of the disease from amyloid pathology to tau pathology, as it occurred without introducing a tau mutation.

However, Nathan and colleagues found that ablation of inducible nitric oxide synthase in the context of an APP mutation resulted in an amelioration of the symptoms and pathology of the Alzheimer's model in mice. A decrease in early mortality and decreased amyloid beta plaque load was found in the mice lacking NOS2 and carrying APP mutations compared to those mice that were wild type for

NOS2. Kummer et al corroborated the results of Nathan et al in 2011. Kummer and colleagues also found a reduced amyloid beta plaque load in mice lacking NOS2. In addition they found that NOS2-/- mice carrying APP mutations demonstrated improved behavior over mice carrying the APP mutation alone. Kummer et al also showed evidence of nitrated Aβ in tissue from Alzheimer's patients and mice, specifically at tyrosine 10. Both Nathan et al and Kummer et al concluded that ablation of inducible nitric oxide synthase offered a protective phenotype. However, both groups studied a transgenic mouse line that expressed mutations in both APP and presenilin 1 genes. Additionally, Nathan and colleagues used a NOS2-/- construct disrupting the NOS2 promoter and exons 1-4 (MacMicking et al, 1995), while the Colton, Wilcock and Kummer groups all used a NOS2-/- strain in which exons 12-13 were disrupted (mice from Jackson laboratories #002609). Therefore, it is possible that presenilin mutation and variable NOS2-/- strains may affect the NOS2-/- phenotype resulting in the amelioration of symptoms observed.

Specific Aims:

In this project I will also be examining the effects of ablating the inducible nitric oxide synthase gene in the context of a mutation in the amyloid precursor protein gene. I will examine several phenotypes of mice carrying the APPSwInd mutation described above**,** in conjunction with a lack of inducible nitric oxide synthase. Among these will be total neuronal levels, levels of phosphorylated tau protein and amyloid plaque load. These parameters will be used to determine the

severity of the disease and ultimately whether the ablation of inducible nitric oxide synthase serves to exacerbate the disease or offers a protective phenotype.

Additionally, mice lacking inducible nitric oxide synthase while carrying the APPSwInd D664A genotype described above will be examined. The phenotypes that were examined for APPSwInd mice will be tested in these mice as well. Again the severity of the disease will be judged by the extent of the phenotypes examined. These mice may indicate whether amyloid beta mediated toxicity proceeds via the amyloid precursor protein and the production of the C31 peptide.

MATERIALS AND METHODS

Animals:

The animals used in this study were generated by mating J20 (APPSwInd), heterozygous mice, purchased from Jackson Laboratories, or B21 (APPSwInd D664A) heterozygous mice, kindly provided by Dr. Veronica Galvan, with mice lacking functional inducible nitric oxide synthase (NOS2-/-) due to deletion of exons 12 and 13, also purchased from Jackson laboratories. The resulting mice with the genotype J20+/-; NOS2+/- were mated to those with the genotype J20-/-; NOS2+/-. The resulting mice with the genotype B21+/-;NOS2+/- were mated with B21-/-; NOS2+/- mice. The mice resulting from this cross were aged until 12-13 months of age and included in the study in six different groups: J20+/-; NOS2-/-, J20+/-; NOS2+/-, J20+/-; NOS2+/+, B21+/-; NOS2-/-, B21+/-; NOS2+/-, and B21+/-; NOS2+/+.

Genotyping:

DNA Extraction:

DNA was extracted from the toes of mice. The toes were immersed in 500 ul of a tail lysis buffer containing 100mM Tris-Hcl (pH8-8.5), 5mM EDTA, 0.2%SDS, and 200mM NaCl with 3ul of proteinase K. The mixture was incubated overnight in a 55^{o}C water bath. The tubes were then agitated by vortex and spun down for 15 minutes at 14,000 rpm at 4^{o}C. Three hundred ul of the solution was added to 300 ul of isopropanol and the DNA was collected on a pipette tip. The DNA was then dissolved in 150 ul of deionized water.

Polymerase Chain Reaction:

In order to determine the presence of the J20 or B21 allele 1 ul of re-suspended DNA was combined with 2 ul of 10X buffer, 0.5 ul of 10mM dNTPs, 1 ul of forward primer (GGT GAG TTT GTA AGT GAT), 1 ul of reverse primer (TCT TCT TCT TCC ACC TCA G), 14.1 ul water, and 0.4 ul of taq DNA polymerase. The PCR protocol required 4 minutes at 94^{o}C, 35 cycles of 20 seconds at 94^{o}C, 30 seconds at 55^{o}C, and 40 seconds at 72^{o}C, followed by 2 minutes at 72^{o}C.

To determine whether there were one, two or zero copies of the inducible nitric oxide synthase gene 3 ul of re-suspended DNA were combined with 2.5 ul of 10X reaction buffer, 16 ul of water, 0.25 ul of wild type forward primer (CCT GTG TTC CAC CAG GAG AT), 0.25 ul of wild type reverse primer (GAG TCA GGA AGG ATG CCT CA), 1 ul of mutant forward primer (ACA TGC AGA ATG AGT ACC GC), 1 ul of mutant reverse primer (AAT ATG CGA AGT GGA CCT CG), 0.5 ul of 10mM dNTPs and 0.5 ul of taq DNA polymerase. The PCR protocol was 3 minutes at 95^{o}C, followed by 40 cycles of 10 seconds at 95^{o}C, 20 seconds at 58^{o}C, and 30 seconds at 72^{o}C.

Brain Collection and Tissue Preparation:

Tissue Collection and Storage:

Mice were anesthetized with isoflurane and perfused intracardially with 100 ml of ice-cold 1X-phosphate buffered saline (PBS). After perfusion the brain was removed and bisected along the sagittal line. The olfactory bulb and cerebellum

were removed from one half of the brain and stored at -80^{o}C. The remaining half of the brain was fixed in 4% paraformaldehyde/4% sucrose at 4^{o}C for 48 hours. The brains were then transferred to a 30% sucrose (in PBS) solution and stored a 4^{o}C for cryoprotection.

Sectioning Fixed Tissue:

After fixation and cryoprotection the brains were removed from the sucrose solution and sectioned by one of two methods. The first method was by frozen microtome (Microm HM 400). The cerebellum was removed and the brain was mounted on a stage. Dry ice and ethanol were added to wells surrounding the stage in order to freeze the brain. The frozen microtome was set to 50-micron slices and the slices were collected serially and stored in PBS in a 24 well plate. The second method used was an agarose-gel machine. The cerebellum of the brain was removed and the brain was mounted in a mold and immersed in a 1% agarose gel. The microtome (Compresstome VF-300 Microtome) was set to 50-micron slices and the brain slices were collected serially in a 24 well plate in PBS.

CHAPSO and Formic Acid Extraction:

The brains (stored at -80^{o}C) were weighed and placed in a Beckman tube (Beckman 349622). One ml of 1% CHAPSO in PBS with 25x protease inhibitor (Roche Complete Protease Inhibition Cocktail) was added to each tube. The brains were then processed with a dounce homogenizer three times over ice for 15 seconds. The homogenates were then incubated at 4 ^{o}C for 30 minutes and centrifuged at 46,000 rpm at 4^{o}C for one hour using a TLA-100.3 rotor (Beckman). The resulting

supernatant was collected and put into 150 ul aliquots. The aliquots were stored at -80^{o}C for later analysis.

One ml of 70% formic acid was added to the pellet remaining from the CHAPSO extraction. The pellets were processed with a dounce homogenizer three times over ice, for 15 seconds each time. The homogenates were then centrifuged at 46,000 rpm at 4^{o}C for one hour using a TLA-100.3 rotor (Beckman). The clear supernatant (located between a pellet and a floating lipid layer) was removed and diluted 9:1 with 2M Tris Base (pH 11.2). The Tris Base was added until the solution was neutralized to an approximate pH of 8-8.5. The resulting solutions were centrifuged at 3000 rpm for 5 minutes and 4^{o}C. The supernatant was collected in 1.5 ml aliquots and stored at -80^{o}C for future analysis.

Immunohistochemistry:

Aβ Staining:

Brain slices (three per animal- one rostral, one mid, and one caudal hippocampus) were mounted on glass slides and allowed to dry overnight. The slides were then washed twice in tris buffered saline (TBS) (5 minutes) and once for three minutes in 88% formic acid. The slides were then washed two additional times with TBS (5 minutes) and once for 30 minutes in a hydrogen peroxide solution (TBS with 10% hydrogen peroxide and 10% methanol). The slides were washed twice in TBS, once for 15 minutes in TBS-A (TBS with 0.1% Triton-X), and once for 30 minutes in TBS-B (TBS with 0.1% Triton-X and 3% Bovine Serum Albumin). An

anti-amyloid beta antibody (69D) was added (1:1000 in TBS-B) and left overnight at 4^{o}C.

Next the slides were washed 3 times (for 5 minutes) in TBS-A and once in TBS-B for 15 minutes. The secondary antibody was a horse anti mouse biotinylated antibody (Vector V0522) (1:200 in TBS-B with 1.5% horse serum) and was applied for 1 hour at room temperature. The slides were washed again with TBS-A (3 times for 5 minutes) and TBS-B (1 time for 15 minutes) before an Avidin-Biotinylated enzyme Complex (ABC) solution (Vectastain Elite Kit by Vector) was applied for 1 hour at room temperature. The slides were washed 5 times with TBS (5 minutes) and then immersed in diaminobenzedine tetrahydrochloride (DAB) for three minutes. The slides were washed 5 additional times in TBS (5 minutes) and dehydrated by successive washes in 50% (3 minutes), 70% (3 minutes), 95% (3 minutes), and 100% ethanol (10 minutes), followed by 2 washes in xylene (1 and 15 minutes respectively). Coverslips were then applied with Depex Media (Electron Microscopy Sciences).

Images of the slides were taken at a 4X objective (Olympus IX81 Microscope). The images were converted to gray scale in ImagePro. The program was then used to determine the percentage of area carrying a positive stain. A threshold was set (used for all slides) and the percentage for the hippocampus was determined. Analysis was performed using a one-way ANOVA with post-hoc Tukey analysis.

Tau Staining:

Brain slices were mounted on glass slides and allowed to dry overnight. The slides were then washed two times with TBS (5 minutes) and once for 30 minutes in a hydrogen peroxide solution (TBS with 10% hydrogen peroxide and 10% methanol). The slides were washed twice in TBS, once for 15 minutes in TBS-A (TBS with 0.1% Triton-X), and once for 30 minutes in TBS-B (TBS with 0.1% Triton-X and 3% Bovine Serum Albumin). An antibody against tau protein phosphorylated at Ser202/Thr205 (AT8 from Pierce antibodies) was added (1:500 in TBS-B) and left overnight at 4^{o}C.

Next the slides were washed 3 times (for 5 minutes) in TBS-A and once in TBS-B for 15 minutes. The secondary antibody was a horse anti mouse biotinylated antibody (Vector V0522) (1:200 in TBS-B with 1.5% horse serum) and was applied for 1 hour at room temperature. The slides were washed again with TBS-A (3 times for 5 minutes) and TBS-B (1 time for 5 minutes) before an Avidin-Biotinylated enzyme Complex (ABC) solution (Vectastain Elite Kit by Vector) was applied for 1 hour at room temperature. The slides were washed 5 times with TBS (5 minutes) and then immersed in diaminobenzedine tetrahydrochloride (DAB) for three minutes. The slides were washed 5 additional times in TBS (5 minutes) and dehydrated by successive washes in 50% (3 minutes), 70% (3 minutes), 95% (3 minutes), and 100% ethanol (10 minutes), followed by 2 washes in xylene (1 and 15 minutes respectively). Coverslips were then applied with Depex Media (Electron Microscopy Sciences).

Western Blot Preparation and Analysis:

Determination of Total Protein:

The total amount of protein per sample was determined using the Pierce Micro BCA Kit. A stock solution was prepared by adding stock solutions A, B, and C in 25:24:1 proportions followed by a 1:1 dilution with de-ionized water. Standards were prepared by adding the following volumes of a 1ug/ul stock solution of bovine serum albumin: 0 ul, 0ul, 1ul, 2.5 ul, 5 ul, 10 ul, 15 ul, 20 ul. Next 1:10 dilutions were made for each of the unknown samples. Ten ul of the unknown samples were transferred to fresh reaction tubes and 1 ml of the BCA stock solution prepared above was added to each of the samples and controls. The tubes were incubated for 20 minutes in a 55^{o}C water bath. The controls were then read at 256 nm using a spectrophotometer (Spectronics Genesys 5) and a standard curve was prepared. The unknown samples were then read at 256 nm and the protein concentration was determined according to the standard curve.

Western Blot Preparation:

The separating gels prepared were 11% acrylamide gels with a 1.4 M Bis/Tris buffer (pH 6.4). The gels were run with 1X MOPS buffer at 70 mV through the stacking gel and 140 mV through the separating gel. The protein was transferred to a 0.45 um nitrocellulose membrane at 380 mA for 1 hour at 4^{o}C. The membrane was blocked for 1 hour in 5% milk in TBS with 0.1% Tween detergent (TBS-T). The membrane was washed with TBS-T and then immersed in the primary antibody (PHF1- anti-phosphorylated tau at ser396/ser404 1:500; 6E10- anti-amyloid beta 1-

16 1:1,000 from Covance Laboratories #9320-02; CT15- anti-C-terminal region of APP 1-15 1:10,000 with 5% milk; E7- anti-β -tubulin1:2,000) overnight at 4^{o}C.

The following morning the membrane was washed with TBS-T (3 times for 15 minutes) and the secondary antibody coupled to horseradish peroxidase was added at 1:2500 with 5 % milk in TBS-T (Goat-anti-mouse was used for PHF1, 6E10, E7, and Tau5; Goat-anti-rabbit was used for CT15) and the membrane was incubated in the solution for 1 hour at room temperature. The membrane was then washed with TBS-T (3 times for 15 minutes) and TBS (one time for 10 minutes). The membrane was then immersed in a Super Signal West Pico Solution (Thermo Scientific) for two minutes. The membrane was then used to expose and develop film. Images were also obtained using a FluorChemQ camera (Cell Biosciences). The optical density of the different lanes was determined using the above program and was analyzed using a one-way ANOVA with post-hoc Tukey analysis.

Enzyme Linked Immunosorbent Assay Aβ40 and Aβ42*:*

A 96-well plate was coated with an anti-N-terminal Aβ1-16 antibody [Ab9 (4.4 ug/ul) provided by Dr. Todd Golde] and incubated overnight at 4^{o}C for Aβ40 ELISA. The coating buffer was removed and 1% blocking solution was added. The plate was incubated overnight at 4^{o}C. Next the blocking solution was removed and the plate was washed several times with PBS. Antigen capture buffer was added to the wells followed by the diluted samples and solutions. The plate was incubated at 4^{o}C overnight. The samples were removed and the plate was washed several times. The secondary antibody was anti-Aβ35-40 (HRP 13.1.1 provided by Dr. Todd Golde) and

was added 1:1000 in PBS with 1% BSA. The plate was incubated at room temperature for 4 hours. The wells were washed with PBS-tween followed by PBS. TMB (Thermo Scientific #34028) was added followed by the stop buffer.

Aβ42 ELISA was performed according to the same protocol using MM26.2.1.3 (provided by Dr. Todd Golde) as the primary antibody at 50ug/ul. The secondary antibody used was HRP coupled 6E10 (anti-Aβ1-16) at 1:1000. Analysis was performed on the groups using one-way ANOVA with post-hoc Tukey tests to determine significance. All ELISA experiments in this report were performed by Hiroko Maruyama.

RESULTS

B21 and J20 mice express human APP and total APP at similar levels

First we checked whether there was any difference in the expression level of the human amyloid precursor protein (hAPP) between mice carrying the B21 or J20 allele. There were no significant differences (according to one way ANOVA with post-hoc Tukey tests; $p>0.05$) in the levels of hAPP as assessed by densitometry analysis of a western blot probed with an antibody specific to the human amyloid beta sequence of APP (6E10) (Figure 3). In addition the presence or absence of the inducible nitric oxide synthase gene did not influence the level of hAPP expression. However, mice carrying the B21 and J20 alleles regardless of inducible nitric oxide synthase expression, displayed significantly lower levels of hAPP than a tgCRND8 mouse (Chishti et al, 2001). Levels of total APP were also examined by western blots labeled with an antibody specific to the C-terminus of the APP protein (CT15). It was determined that there were comparable levels of APP expression among the B21+/- and J20+/- mice. The optical density of the western blots was compared to a positive control TgCRND8 mouse, which produces plaques as early as 3 months (Chishti et al, 2001).

A.

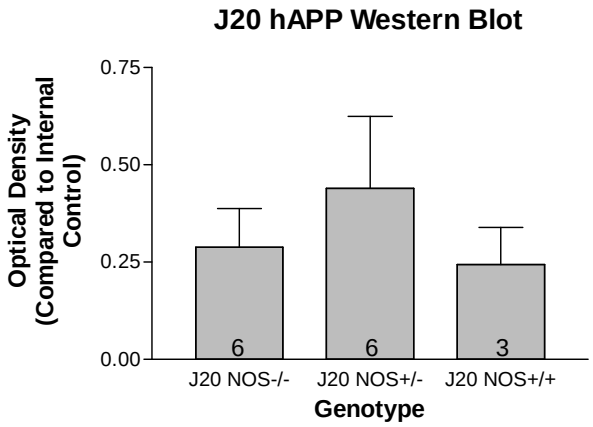

B.

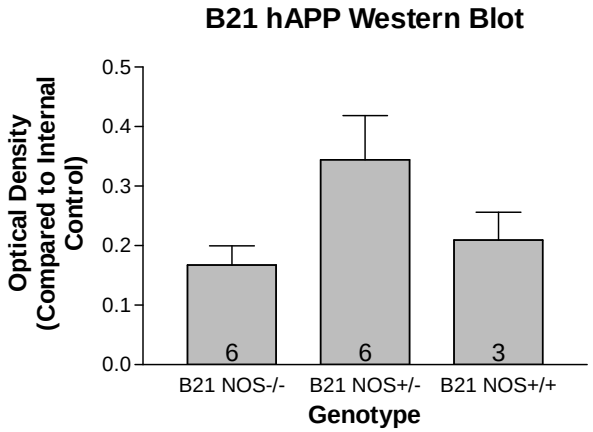

Figure 3: Western blot quantification for hAPP

Western blot quantifications are shown. Optical density was normalized to a control and quantified ($p>0.05$).

Inducible nitric oxide synthase expression does not affect the production of amyloid beta

Next we examined the levels of insoluble amyloid beta via ELISA of formic acid brain extractions (performed by Hiroko Maruyama) in order to assess the levels of deposited Aβ. There was no significant difference ($p>0.05$) between J20+/-; NOS2-/-, J20+/-; NOS2+/-, and J20+/-; NOS2+/+ mice in the levels of amyloid-beta 40 or 42 in formic acid fractions (figure 4). Similarly no significant differences (according to one-way ANOVA analysis with post-hoc Tukey tests; $p>0.05$) were observed in the levels of amyloid-beta 40 or 42 among B21+/-; NOS2-/-, B21+/-, NOS2+/-, and B21+/-; NOS2+/+ mice (figure 5).

B21 and J20 mice showed low levels of amyloid plaques

Brain slices perfused with phosphate buffered saline were stained using an anti-amyloid beta antibody (69D) in order to assess the plaque load in the animals (figures 6-7). The levels were then determined using a threshold analysis. There were no significant differences ($p>0.05$) between J20+/-; NOS2-/-, J20+/-; NOS2+/-, and J20+/-; NOS2+/+ mice (figure 8A). There was however a significant difference ($p<0.05$) in the amyloid plaque load between B21+/-; NOS2-/- and B21+/-; NOS2+/- mice. There were no significant differences between either of the above groups and the B21+/-; NOS2+/+ group (figure 8B). However, there were clearly two outliers raising the average for the B21+/-; NOS2-/- as seen in figure 9.

A.

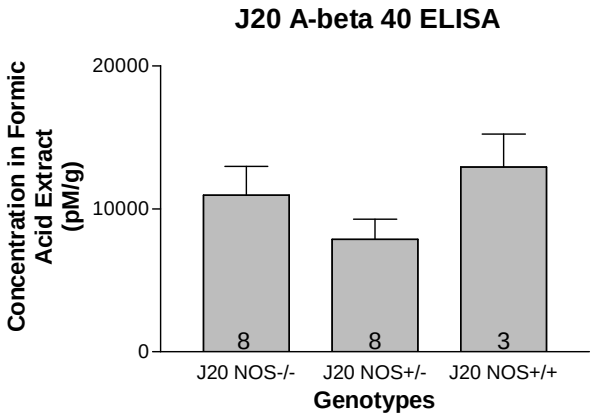

B.

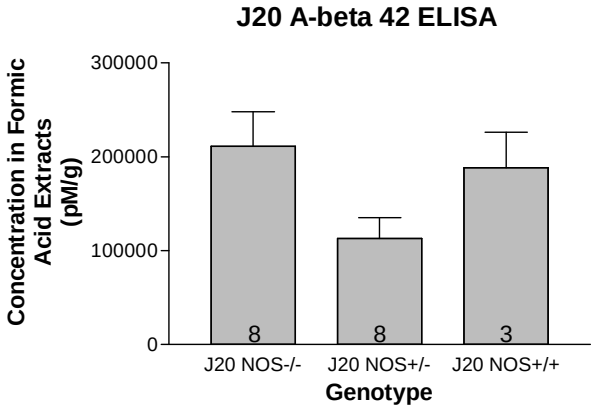

Figure 4: Levels of insoluble amyloid-beta protein in J20 mice

Amount of insoluble amyloid-beta protein in J20 mice as measured in formic acid extract fractions by ELISA. Figure 4A shows the levels of amyloid-beta 40 while figure 4B shows the levels of amyloid-beta 42 ($p>0.05$).

A.

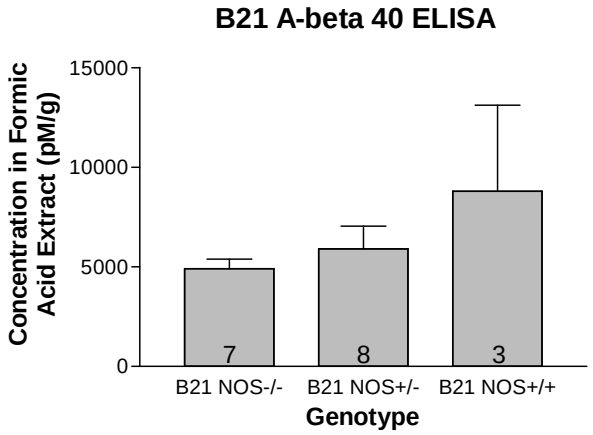

B.

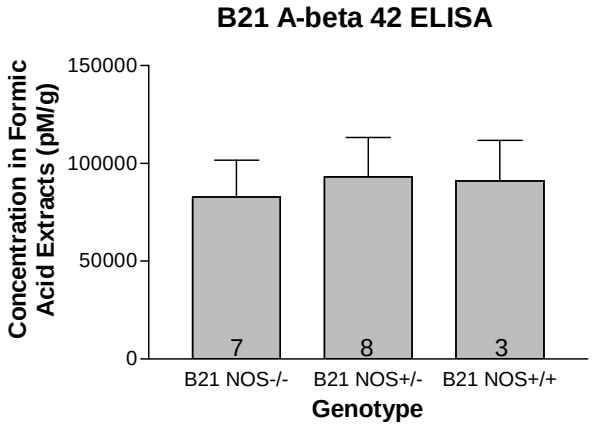

Figure 5: Levels of insoluble amyloid-beta protein in B21 mice

Amount of insoluble amyloid-beta protein in B21 mice as measured in formic acid extract fractions by ELISA. Figure 5A shows the levels of amyloid-beta 40 while figure 5B shows the levels of amyloid-beta 42 ($p>0.05$).

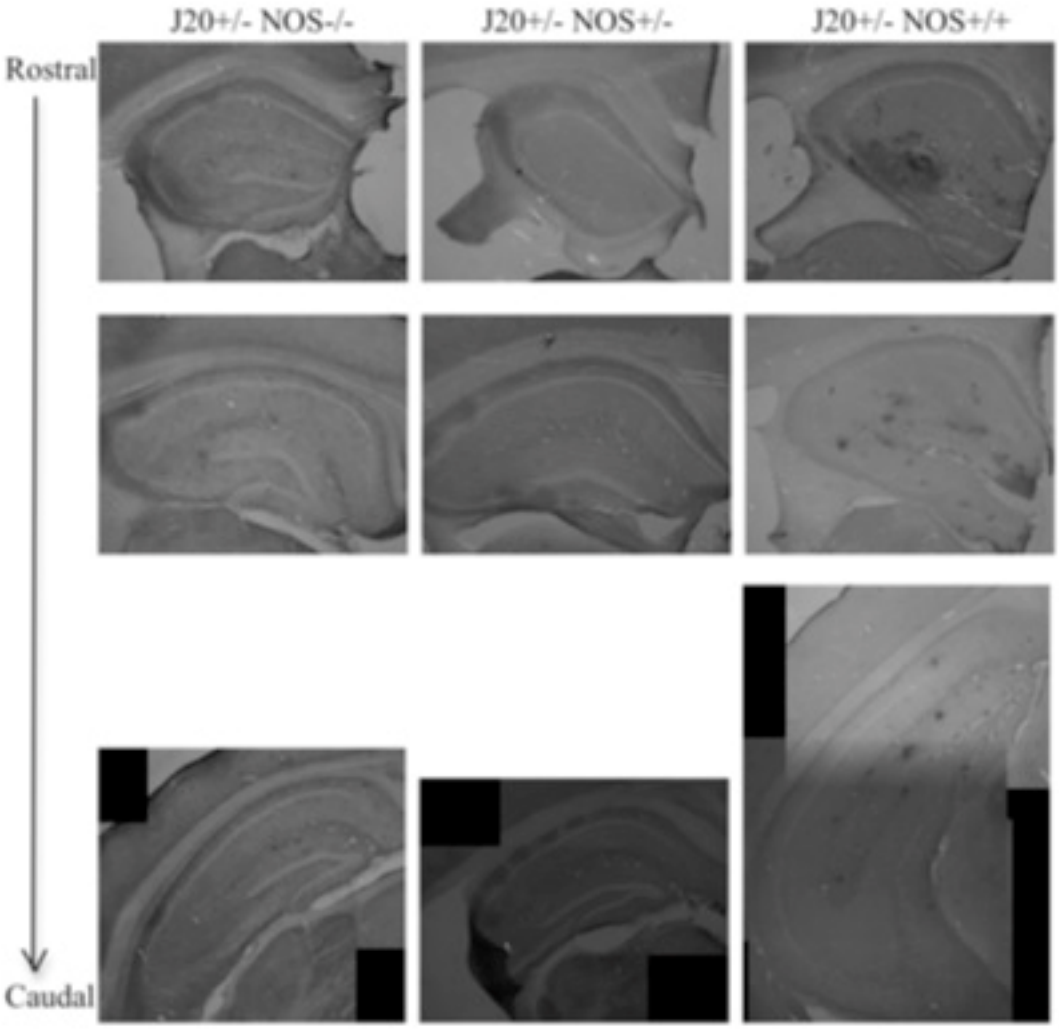

Figure 6: Images of brain slices immunostained for amyloid-beta

Representative images of immunohistochemistry staining of brain slices. The antibody used (69D) detects amyloid plaques. The images, moving from left to right are of J20+/-; NOS-/-, J20+/-; NOS+/-, and J20+/-; NOS+/+. Moving from top to bottom the images are from the rostral side of the brain towards the caudal end.

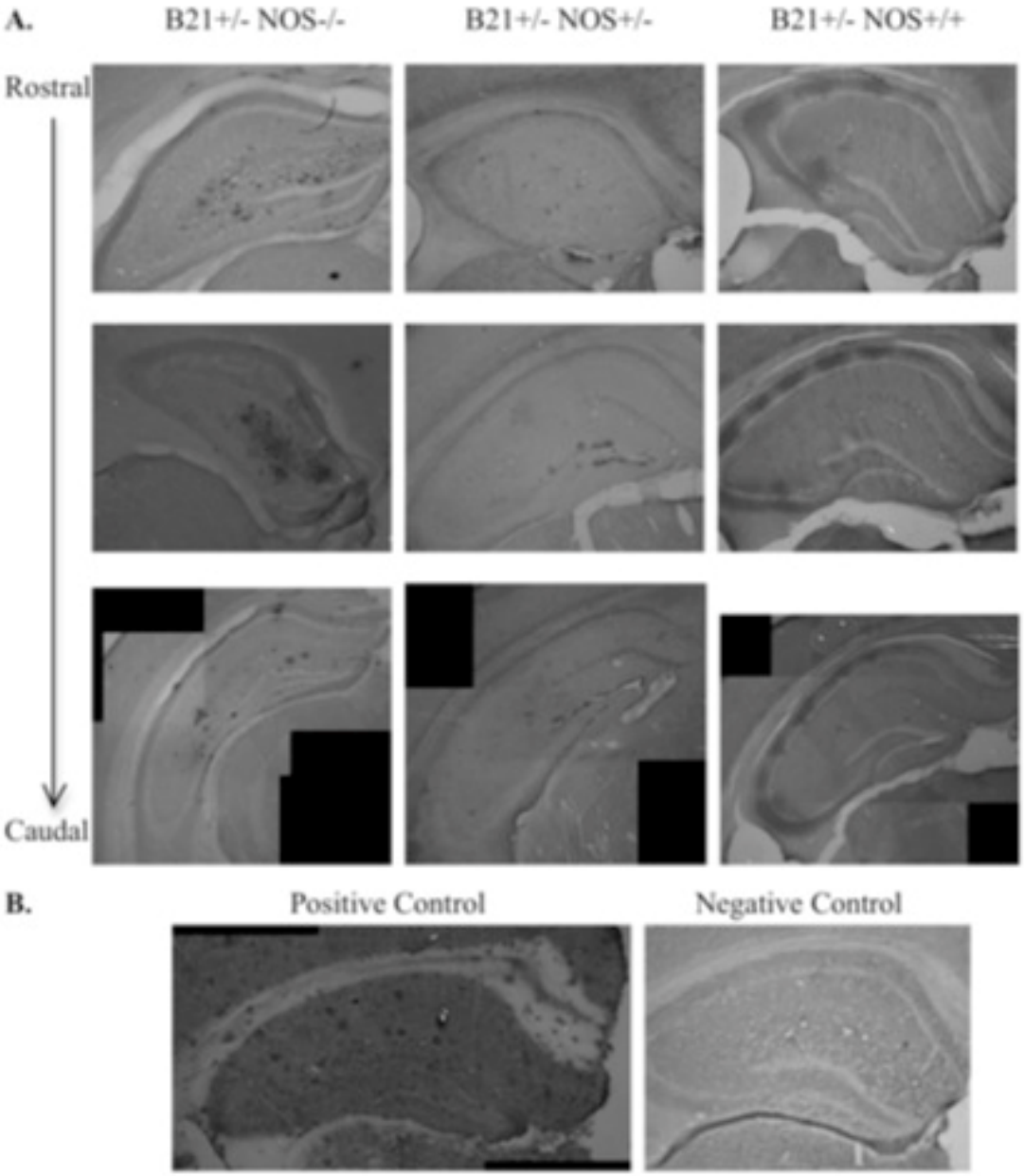

Figure 7: Images of brain slices immunostained for amyloid-beta

Representative images of immunohistochemistry staining of brain slices. The antibody used (69D) detects amyloid plaques. The images, moving from left to right are of B21+/-; NOS-/-, B21+/-; NOS+/-, and B21+/-; NOS+/+. Moving from top to bottom the images are from the rostral side of the brain towards the caudal end (7A). The positive control brain and a non-transgenic negative control are also shown (7B).

A.

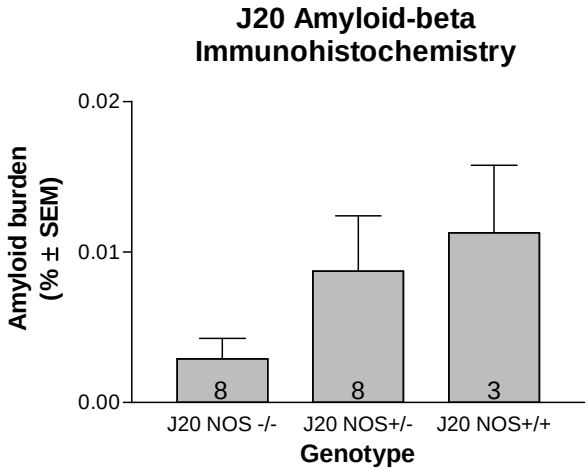

B.

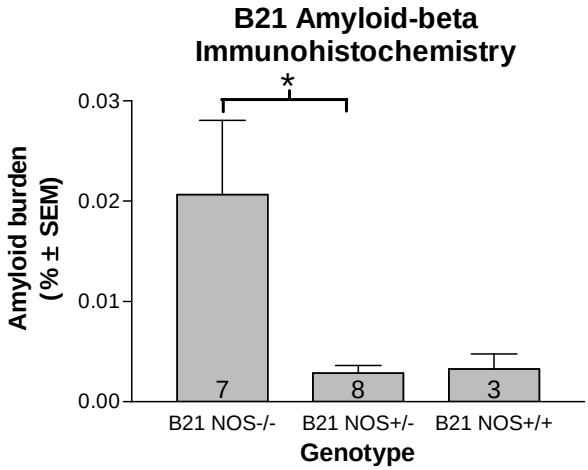

Figure 8: Quantification of 69D images

The above figures indicate the percentage of area that showed a positive stain for amyloid plaques. Figure 8A shows the J20+/- group ($p>0.05$) and figure 8B shows the B21+/- groups. (* indicates $p<0.05$).

A.

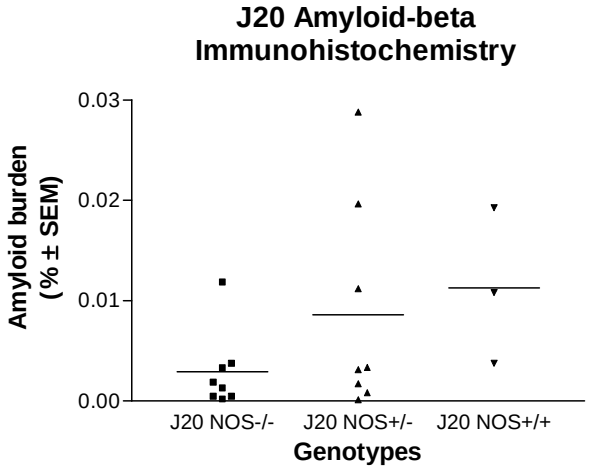

B.

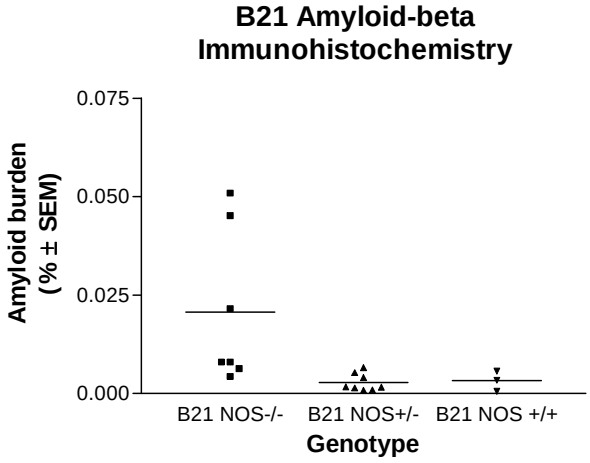

Figure 9: Individual levels of amyloid-positive stain

The distribution of mice used to determine the levels of amyloid plaque load in figure 8.

Inducible nitric oxide synthase expression does not alter levels of hyperphosphorylated tau protein

Finally we assessed the levels of hyperphosphorylated tau among the groups. Brain slices immunostained with an anti-phosphorylated tau antibody (AT8) indicated that only one brain out of 34 examined displayed positive hyperphosphorylated tau (figures 11-13). The animal that displayed the tau staining was a B21+/-; NOS2-/- mouse. In addition levels of hyperphosphorylated tau were assessed via western blot analysis using an anti-phosphorylated tau antibody (PHF1) (figure 10A). There were no significant differences observed between the J20+/-; NOS2-/-, J20+/-; NOS2+/-, and J20+/-; NOS2+/+ mice (figure 10B). Similarly no significant differences were observed between the B21+/-; NOS2-/-, B21+/-; NOS2+/-, and B21+/-; NOS2+/+ groups (figure 10C). The PHF1 antibody was used for western blot analysis after the AT8 antibody repeatedly produced no signal on the blots.

A.

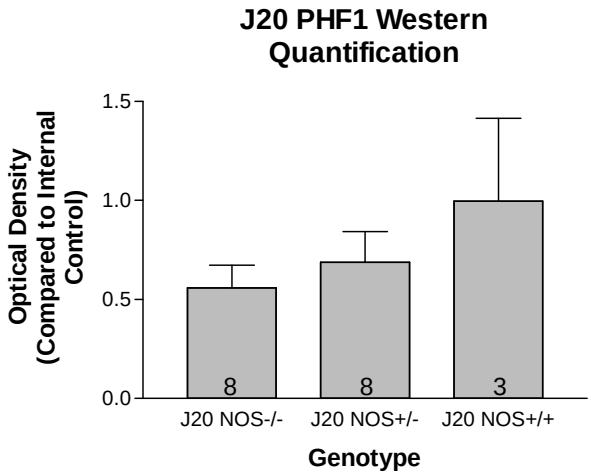

B.

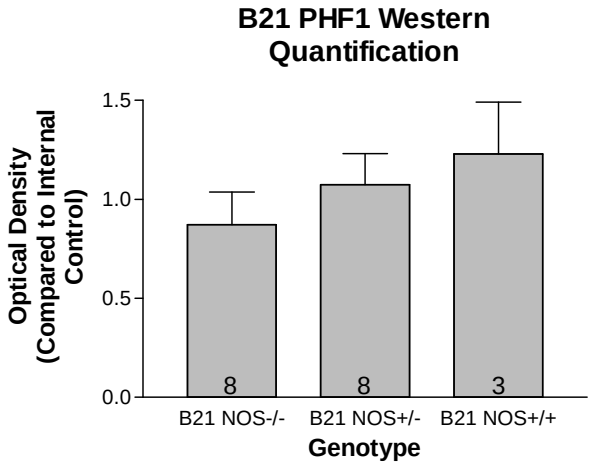

Figure 10: Western quantification for hyperphosphorylated tau

Western blot quantifications are shown. Optical density was normalized to a control and quantified ($p>0.05$)

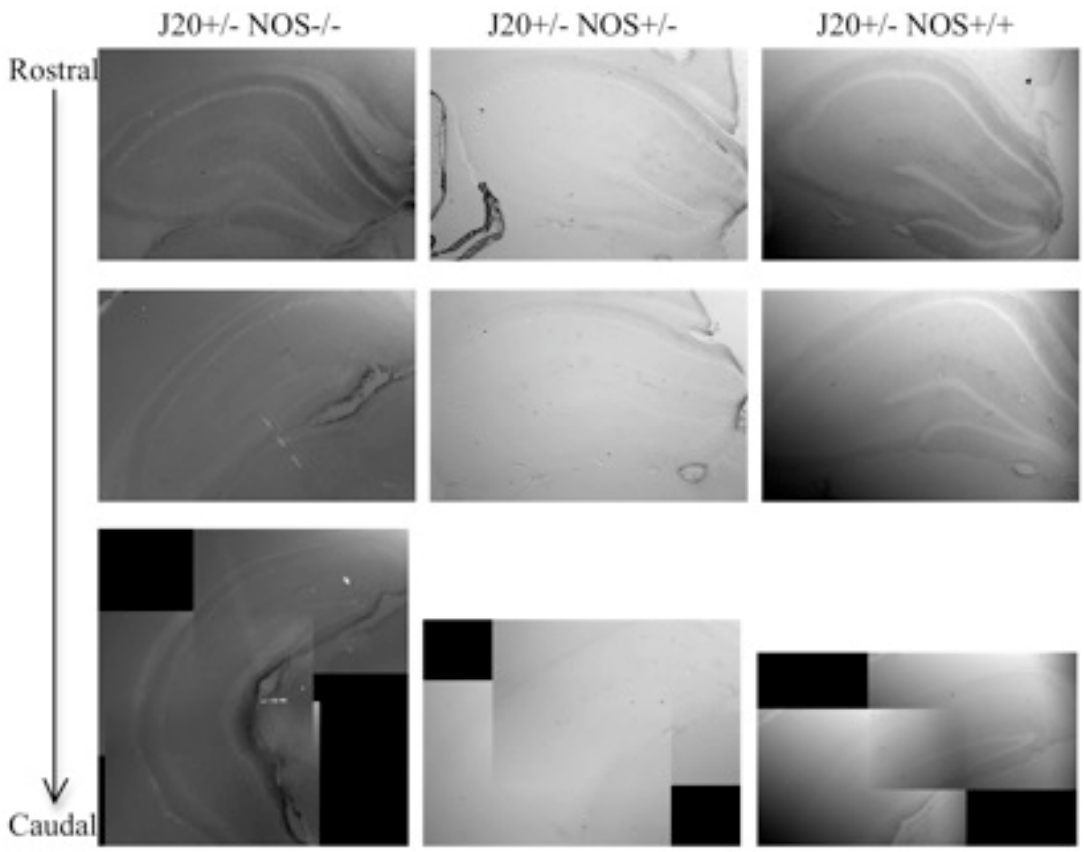

Figure 11: Images of brain slices immunostained for hyperphosphorylated tau

Representative images of immunohistochemistry staining of brain slices. The antibody used (AT8) detects hyperphosphorylated tau. The images, moving from left to right are of J20+/-; NOS-/-, J20+/-; NOS+/-, and J20+/-; NOS+/+. Moving from top to bottom the images are from the rostral side of the brain towards the caudal end.

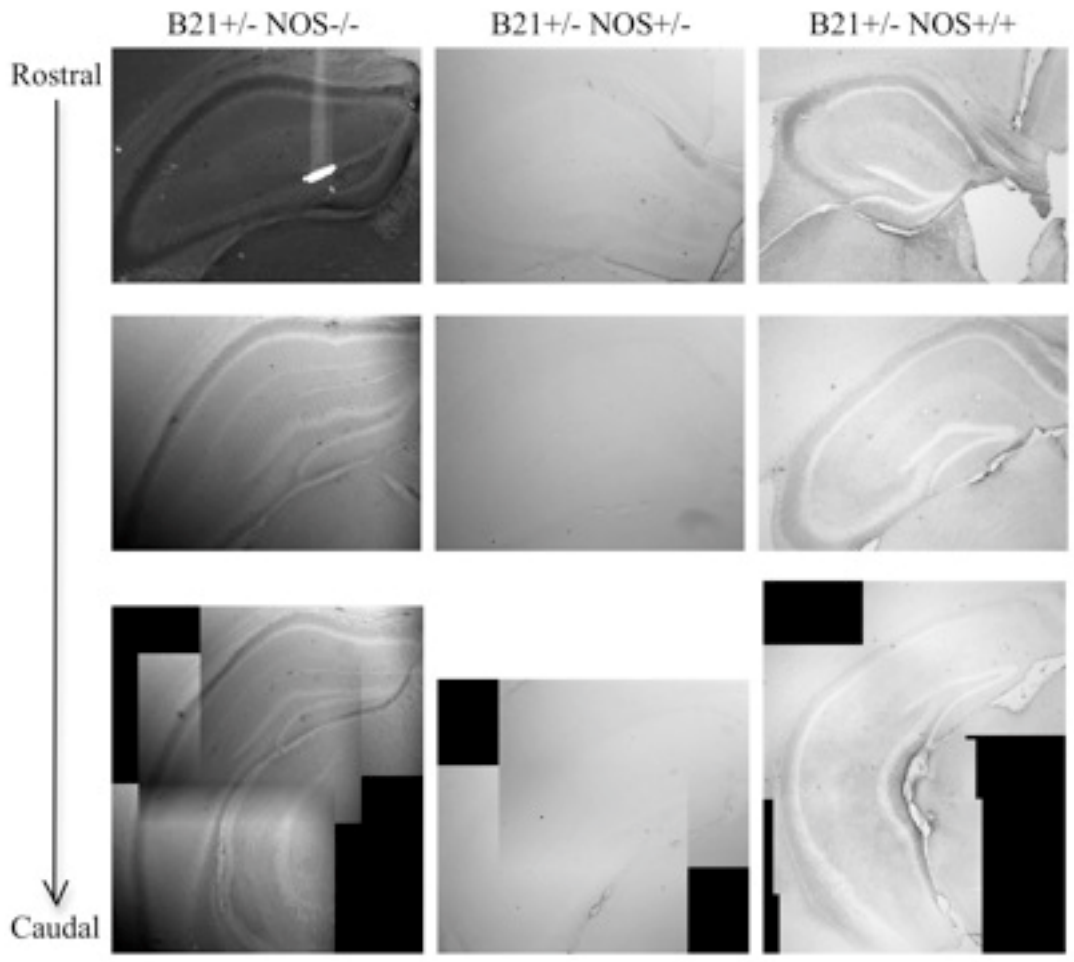

Figure 12: Images of brain slices immunostained for hyperphosphorylated tau

Representative images of immunohistochemistry staining of brain slices. The antibody used (AT8) detects hyperphosphorylated tau. The images, moving from left to right are of B21+/-; NOS-/-, B21+/-; NOS+/-, and B21+/-; NOS+/+. Moving from top to bottom the images are from the rostral side of the brain towards the caudal end.

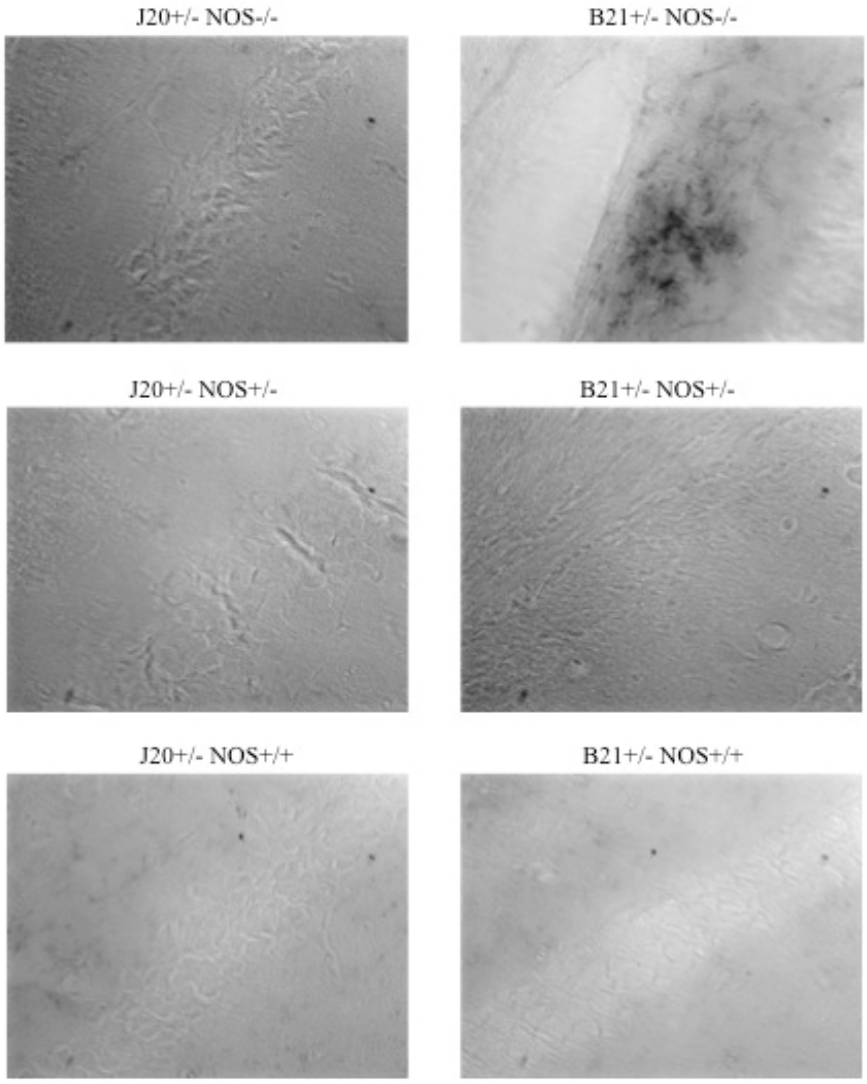

Figure 13: High magnification images of brain slices immunostained for hyperphosphorylated tau

Representative images of immunohistochemistry staining of brain slices. The antibody used (AT8) detects hyperphosphorylated tau. The images were taken using a 40X objective in the CA1 region of the mid hippocampus.

DISCUSSION

Our first goal was to confirm that the mice carrying the J20 and B21 transgenes continued to express the human amyloid precursor protein transgene with or without the endogenous iNOS gene. Indeed, the transgenic mice showed the expected increase expression of hAPP by western blot analysis. Furthermore, the ablation of inducible nitric oxide synthase did not alter the levels of hAPP. This indicated that any significant changes in the amyloid burden or levels of hyperphosphorylated tau could not be attributed to varying expression of hAPP among the groups.

Next we examined the levels of insoluble amyloid beta (40 and 42) via ELISA. The results indicated that there were no significant differences in the levels between groups. Mice carrying the J20 and B21 transgenes were similar in amyloid expression regardless of the presence (or absence) of inducible nitric oxide synthase. This indicated that the ablation of iNOS did not contribute to increasing amyloid expression or production, nor did it offer a protective phenotype.

Surprisingly, amyloid burden assessed by immunostaining of amyloid deposits in brain did not confirm the ELISA results. The mice expressing the J20 transgene did not show any significant differences in the amyloid plaque burden between the NOS2 genotypes. This indicated that the absence of inducible nitric oxide synthase did not alter the deposition of amyloid plaques in mice aged 12-13 months. However, mice carrying the B21 transgene in the absence of inducible nitric oxide synthase did show a statistically significant increase in amyloid plaque burden. This increase seemed to

be largely dependent on two mice and may be an effect of small sample sizes. Further studies incorporating larger numbers of mice would be needed to confirm the findings.

It is important to note that the levels of amyloid expression, as determined by ELISA and immunohistochemistry, are below the expected values for mice carrying the APPSwInd transgene. This can be seen by comparison of amyloid staining of mice carrying the APPSwInd transgene at 8-9 months old from Mucke et al (2000) and the amyloid staining of mice aged 12-13 months carrying the same transgene in this study (Figure 14).

A.

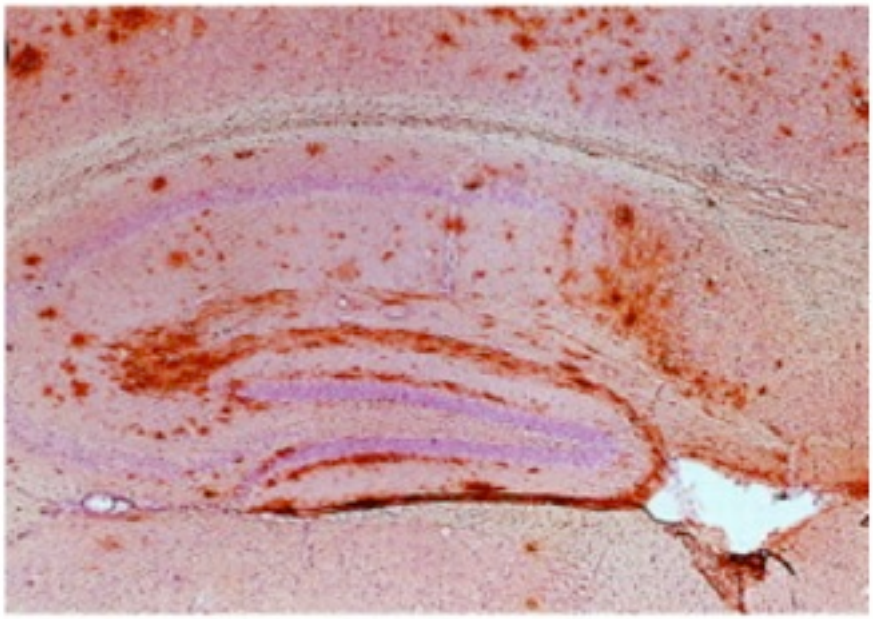

B.

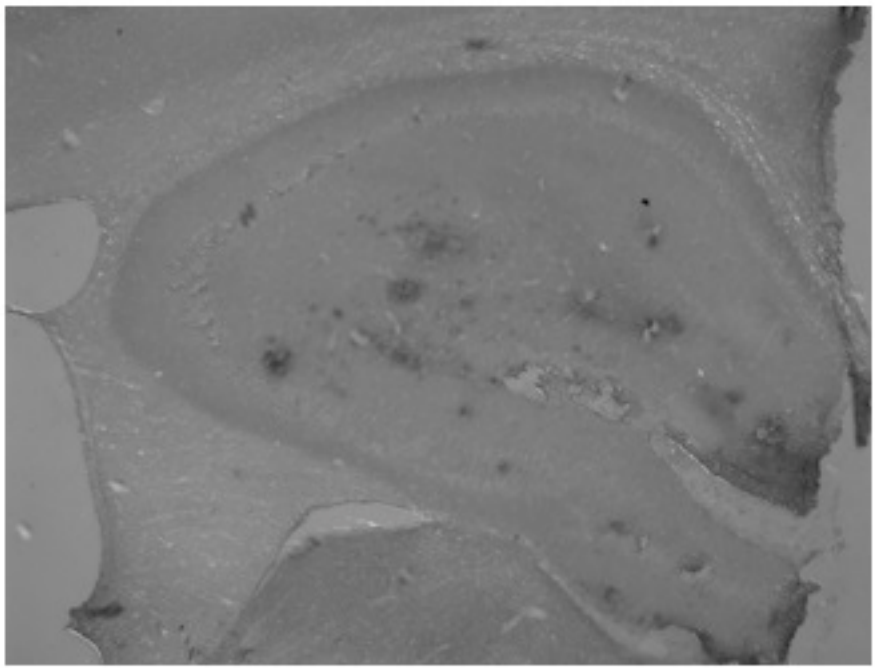

Figure 14: Differing plaque loads between J20 NOS+/+ mice

Amyloid beta staining in original J20 mice (10A) and J20 mice included in this study (10B). Figure 10A is adapted from Mucke et al, 2000.

Finally we examined the levels of hyperphosphorylated tau. Here there were no significant differences observed between the groups, as determined by western blot analysis. In addition very little immune-reactivity was observed by immunohistochemistry analysis. This indicated that the ablation of inducible nitric oxide synthase did not significantly alter the phosphorylation of the tau protein as was reported by the Colton laboratory. Together, the absence of alteration in either the hyperphosphorylated tau levels and the production and deposition of amyloid-beta indicate that mice carrying the J20 transgene did not display any changes in disease progression based on the ablation of inducible nitric oxide synthase. Mice carrying the B21 transgene did not show differences in level of hyperphosphorylated tau or the production of amyloid beta. There was however an increase in the deposition of amyloid beta into plaques, though this is most likely driven by the two outlying mice discussed above.

These results are not consistent with the findings of Colton et al (2006, 2009) and Wilcock et al (2009), which indicated that the ablation of inducible nitric oxide synthase promoted Alzheimer's like pathologies. The results are also inconsistent with the results of Nathan et al (2005) and Kummer et al (2011), which indicated that the ablation of inducible nitric oxide synthase resulted in a protective phenotype. The wide spectrum of results in these studies may indicate that iNOS plays a complicated role in AD progression that is influenced by many factors, that may not yet be known. Although we set out to test whether loss of the caspase cleavage site of APP may have consequences on the predicted tau pathology in the absence of iNOS, this test could

not be done because we could not replicate the elevation of hyperphosphorylated tau pathology that was reported in the setting of “conventional” APP transgenic mice. It is also interesting to note that the levels of hyperphosphorylated tau observed in Colton et al (2006), seemed to vary greatly among APPSwNOS2-/- mice (figure 15). In conclusion, it may necessary to incorporate larger numbers of mice to account for the apparent variation in the phenotype of mice lacking inducible nitric oxide synthase. Given this a larger study incorporating more mice needs to be performed using mice with the APPSwe mutation and deletion of exons 12-13 of iNOS. This will ensure that the results can be compared to those of Colton and colleagues (2006).

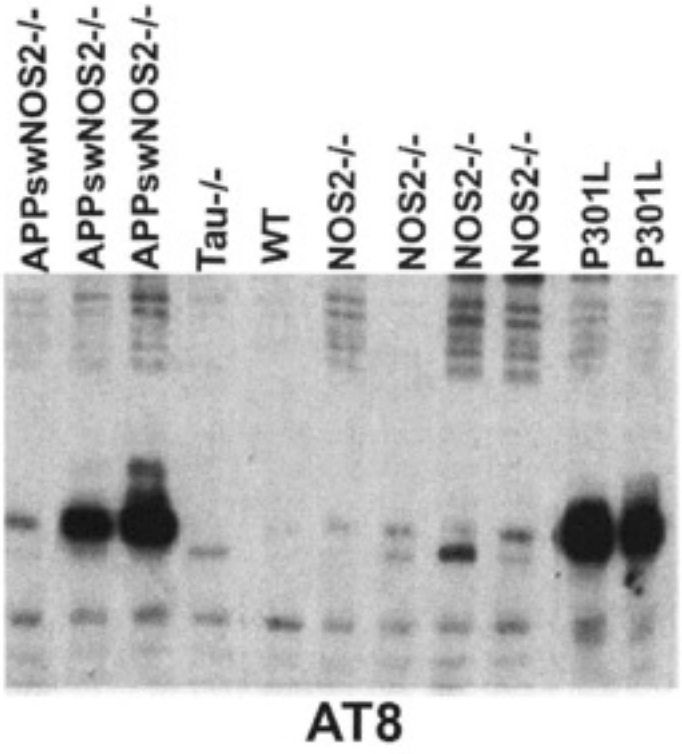

Figure 15: Variable levels of hyperphosphorylated tau protein

Western blot showing the levels of hyperphosphorylated tau in APPswNOS2-/- mice. This figure is adapted from Colton et al, 2006.

REFERENCES

Alzheimer's Association (2011), 2011 Alzheimer's facts and figures. Alzheimer's and Dementia. *7*, 208-244.

Anstey KJ, von Sanden C, Salim A, O'Kearney R (2007). Smoking as a risk factor for dementia and cognitive decline: a meta-analysis of prospective studies. American Journal of Epidemiology. *166(4),*367-78.

Binder, L.I., Guillozet-Bongaarts, A.L. Garcia-Sierra, F., Berry, R.W. (2005). Tau Tangles and Alzheimer's Disease. *1739 (2-3),* 216-223.

Chishti MA, Yang DS, Janus C, Phinney AL, Horne P, Pearson J, Strome R, Zuker N, Loukides J, French J, Turner S, Lozza G, Grilli M, Kunicki S, Morissette C, Paquette J, Gervais F, Bergeron C, Fraser PE, Carlson GA, George-Hyslop PS, Westaway D (2001). Early-onset amyloid deposition and cognitive deficits in transgenic mice expressing a double mutant form of amyloid precursor protein 695. The Journal of Biological Chemistry. *276(24),* 21562-70.

Colton, C.A., Vitek, M.P., Wink, D.A., Xu, Q., Cantillana, V., Previti, M.L., Van Nostrand, W.E., Weinber, J.B., Dawson, H. (2006) NO Synthase 2 (NOS2) deletion promotes multiple pathologies in a mouse model of Alzheimer's disease. Proceedings of the National Academy of Science. *103(34),* 12867-12872.

Colton, C.A., Wilcock, D.M., Wink, D.A., Davis, J., Van Nostrand, W.E., Vitek, M.P. (2008). The Effects of NOS2 Gene Deletion on Mice Expressing Mutated Human AβPP. J. Alzheimer's Disease. Biochimica et Biophysica Acta (BBA) - Molecular Basis of Disease. *15(4),* 571-587.

Cramer PE, Cirrito JR, Wesson DW, Lee CY, Karlo JC, Zinn AE, Casali BT, Restivo JL, Goebel WD, James MJ, Brunden KR, Wilson DA, Landreth GE (2012). ApoE-directed therapeutics rapidly clear β-amyloid and reverse deficits in AD mouse models. Science. *335(6075),*1503-6.

Diagnostic and Statistical Manual of Mental Disorders, Fourth Edition, Text Revision (DSM-IV-TR)

Downen M, Zhao ML, Lee P, Weidenheim KM, Dickson DW, Lee SC (1999). Neuronal nitric oxide synthase expression in developing and adult human CNS. Journal of Neuropathology and Experimental Neurology. *58(1),* 12-21.

Fernandez AP, Pozo-Rodrigalvarez A, Serrano J, Martinez-Murillo R (2010). Nitric oxide: target for therapeutic strategies in Alzheimer's disease. Current Pharmaceutical Designs. *16(25),* 2837-50.

Goedert, M., Spillantini, M.G., Davies S.W., (1998). Filamentous Nerve Cell Inclusions in Neurodegenerative Diseases. Current Opinion in Neurobiology. *8,* 619-632.

Golde, T.E., Schneider, L.S., Koo, E.H. (2011). Anti- Aβ Therapeutics in Alzheimer's Disease: The Need for a Paradigm Shift. Neuron. *69(2),* 203-13.

Hardy, J., Selkoe D.J. (2002). The Amyloid Hypothesis of Alzheimer's Disease: Progress and Problems on the Road to Therapeutics. Science. *297 (5580),* 353-356.

Hartlage-Rübsamen M, Apelt J, Schliebs R (2001). Fibrillary beta-amyloid deposits are closely associated with atrophic nitric oxide synthase (NOS)-expressing neurons but do not upregulate the inducible NOS in transgenic Tg2576 mouse brain with Alzheimer pathology. Neuroscience Letters. *302(2-3),* 73-6.

Hsia AY, Masliah E, McConlogue L, Yu GQ, Tatsuno G, Hu K, Kholodenko D, Malenka RC, Nicoll RA, Mucke L (1999). Plaque-independent disruption of neural circuits in Alzheimer's disease mouse models. Proceedings of the National Academy of Sciences of the United States of America. *96(6),* 3228-33.

Hsiao K, Chapman P, Nilsen S, Eckman C, Harigaya Y, Younkin S, Yang F, Cole G (1996). Correlative memory deficits, Abeta elevation, and amyloid plaques in transgenic mice. Science. *274(5284),*99-102.

Hu J, el-Fakahany EE (1993). beta-Amyloid 25-35 activates nitric oxide synthase in a neuronal clone. Neuroreport. *4(6),* 760-2.

Iqbal K, Alonso Adel C, Chen S, Chohan MO, El-Akkad E, Gong CX, Khatoon S, Li B, Liu F, Rahman A, Tanimukai H, Grundke-Iqbal I (2005). Tau pathology in Alzheimer disease and other tauopathies. Biochimica et Biophysica Acta. *1739(2-3),* 198-210.

Karl T, Bhatia S, Cheng D, Kim WS, Garner B (2012). Cognitive phenotyping of amyloid precursor protein transgenic J20 mice. Behavioural Brain Research. *228(2),* 392-7.

Kivipelto M, Ngandu T, Fratiglioni L, Viitanen M, Kåreholt I, Winblad B, Helkala EL, Tuomilehto J, Soininen H, Nissinen A (2005). Obesity and vascular risk factors at

midlife and the risk of dementia and Alzheimer's disease. Archives of Neurology. *62(10),* 1556-60.

Kummer, M.P., Hermes, M., Delekarte, A., Hammerschmidt, T., Kumar, S., Terwel, D., Walter, J., Pape, H.C., Konig, S., Roeber, S., Jessen, F., Klockgether, T., Korte, M., Heneka, M.T. (2011). Nitration of Tyrosine 10 Critically Enhances Amyloid-β Aggregation and Plaque Formation. Neuron. *71(5),* 833-44.

Lorenzo, A., Yuan, M., Zhang, Z., Paganetti, P.A., Sturchler- Pierrat, C., Staufenbiel, M., Mautino, J., Sol Vigo, F., Sommer, B., Yankner, B.A. (2000). Amyloid Beta Interacts with the Amyloid Precursor Protein: A Potential Toxic Mechanism in Alzheimer's Disease. Nat. Neuroscience. *3(5)*. 460-464.

Lu DC, Rabizadeh S, Chandra S, Shayya RF, Ellerby LM, Ye X, Salvesen GS, Koo EH, Bredesen DE (2000) A second cytotoxic proteolytic peptide derived from amyloid beta-protein precursor. Nat Med. *6*:397– 404.

Lu DC, Soriano S, Bredesen DE, Koo EH (2003) Caspase cleavage of the amyloid precursor protein modulates amyloid beta-protein toxicity. J Neurochem. *87*:733–741.

Lye TC, Shores EA (2000). Traumatic brain injury as a risk factor for Alzheimer's disease: a review. Neuropsychology Review. *10(2),*115-29.

MacMicking, J.D., Nathan, C., Horn, G., Chartrain, N., Fletcher, D.S., Trumbauer, M., Stevens, K., Xie, Q., Sokol, K., Hutchinson, N., Chen, H., Mudgett, J.S. (1995). Altered Responses to Bacterial Infection and Endotoxic Shock in Mice Lacking Inducible Nitric Oxide Synthase. Cell. *81*, 641-50.

Markesbery WR (1997). Neuropathological criteria for the diagnosis of Alzheimer's disease. Neurobiology of Aging. *18(4 Suppl),* S13-9.

Mayeux R, Sano M, Chen J, Tatemichi T, Stern Y (1991). Risk of dementia in first-degree relatives of patients with Alzheimer's disease and related disorders. Archives of Neurology. *48(3),* 269-73.

McGeer PL, McGeer EG (1999). Inflammation of the brain in Alzheimer's disease: implications for therapy. Journal of Leukocyte Biology. *65(4),* 409-15.

Moncada S, Higgs A (1993). The L-arginine-nitric oxide pathway. The New England Journal of Medicine. *329(27),* 2002-12.

Mucke L, Masliah E, Yu GQ, Mallory M, Rockenstein EM, Tatsuno G, Hu K, Kholodenko D, Johnson-Wood K, McConlogue L (2000). High-level neuronal

expression of abeta 1-42 in wild-type human amyloid protein precursor transgenic mice: synaptotoxicity without plaque formation. The Journal of Neuroscience: The Official Journal of the Society for Neuroscience. *20(11)*, 4050-8.

Nathan C (1992). Nitric oxide as a secretory product of mammalian cells. FASEB Journal: The official Publication of the Federation of American Societies for Experimental Biology. *6(12)*, 3051-64.

Nathan C, Xie QW (1994). Nitric oxide synthases: roles, tolls, and controls. Cell. *78(6)*, 915-8.

Nathan C, Xie QW (1994). Regulation of biosynthesis of nitric oxide. The Journal of Biological Chemistry. *269(19),13725-8*.

Nathan, C., Calingasan, N., Nezezon, J., Ding, A., Lucia, M.S., La Perle, K., Fuortes, M., Lin, M., Ehrt, S., Kwon, N.S., Chen, J., Vodovotz, Y., Kipiani, K., Beal, M.F. (2005). Protection from Alzheimer's-like Disease in the Mouse by Genetic Ablation of Inducible Nitric Oxide Synthase. J Exp Med. *202(9)*, 1163-1169.

Oddo, S., Caccamo, A., Shepherd, J.D., Murphy, M.P., Golde, T.E., Kayed, R., Metherate, R., Mattson, M.P., Akbari, Y., LaFerla, F.M. (2003). Triple-Transgenic Model of Alzheimer's Disease with Plaques and Tangles: Intracellular Aβ and Synaptic Dysfunction. Neuron. *39(3)*, 409-21.

Perl DP (2010). Neuropathology of Alzheimer's disease. The Mount Sinia Journal of Medicine. *77(1)*, 32-42.

Polidori MC, Praticó D, Mangialasche F, Mariani E, Aust O, Anlasik T, Mang N, Pientka L, Stahl W, Sies H, Mecocci P, Nelles G (2009). High fruit and vegetable intake is positively correlated with antioxidant status and cognitive performance in healthy subjects. Journal of Alzheimer's Disease. *17(4)*,921-7.

Radde, R., Duma, C., Goedert, M., Jucker, M. (2008). The Value of Incomplete Mouse Models of Alzheimer's Disease. Eur J Nucl Med Mol Imaging. *35 (Suppl 1)*, S70-S74.

Saganich, M.J., Schroeder, B.E., Galvan, V., Bredesen, D.E., Koo, E.H., Heinemann, S.F. (2006). Deficits in Synaptic Transmission and Learning in Amyloid Precursor Protein (APP) Transgenic Mice Require C-Terminal Cleavage of APP. The J of Neuroscience. *26(52)*, 13428-13436.

Salloway S, Mintzer J, Weiner MF, Cummings JL (2008). Disease-modifying therapies in Alzheimer's disease. Alzheimer's and Dementia: The Journal of the Alzheimer's Association. *4(2),*65-79.

Salomone S, Caraci F, Leggio GM, Fedotova J, Drago F (2012). New pharmacological strategies for treatment of Alzheimer's disease: focus on disease modifying drugs. British Journal of Clinical Pharmacology. *73(4),*504-17.

Tsivgoulis G, Alexandrov AV, Wadley VG, Unverzagt FW, Go RC, Moy CS, Kissela B, Howard G (2009). Association of higher diastolic blood pressure levels with cognitive impairment. Neurology. *73(8),*589-95.

Vincent SR (1994). Nitric oxide: a radical neurotransmitter in the central nervous system. Progress in Neurobiology. *42(1),* 129-60.

Vodovotz Y, Lucia MS, Flanders KC, Chesler L, Xie QW, Smith TW, Weidner J, Mumford R, Webber R, Nathan C, Roberts AB, Lippa CF, Sporn MB (1996). Inducible nitric oxide synthase in tangle-bearing neurons of patients with Alzheimer's disease. The Journal of Experimental Medicine. *184(4),* 1425-33.

Wallace MN, Geddes JG, Farquhar DA, Masson MR (1997). Nitric oxide synthase in reactive astrocytes adjacent to beta-amyloid plaques. Experimental Neurology. *144(2),* 266-72.

Wilcock, D.M., Lewis, M.R., Van Nostrand, W.E., Davis, J., Previti, M.L., Gharkholonarhe, N., Vitek, M.P., Colton, C.A. (2008). Progression of Amyliod Pathology to Alzheimer's Pathology in an APP Transgenic Mouse Model by Removal of NOS2. J Neuroscience. *28(7),* 1537-1545.

Wimo, A., Jonsson, L., Gustavsson, A., McDaid, D., Ersek, K., George, J., Gulacsi, L., Karpati, K., Kenigsberg, P., Valtonen, H. (2010). The Worldwide Societal Costs of Dementia: Estimates for 2009. Alzheimer's and Dementia. *6*. 98-103.

Xu WL, Atti AR, Gatz M, Pedersen NL, Johansson B, Fratiglioni L (2011). Midlife overweight and obesity increase late-life dementia risk: a population-based twin study. Neurology. *76(18),* 1568-74.

Zheng, H., Koo, E.H. (2011). Biology and Pathophysiology of the Amyloid Precursor Protein. Molecular Neurodegeneration. *6(1),* 27.